

FIGURE 8.3.31 Wall temperature effect on an oblique shock reflection at $M_\infty = 2.4$ (Délery, 1992).

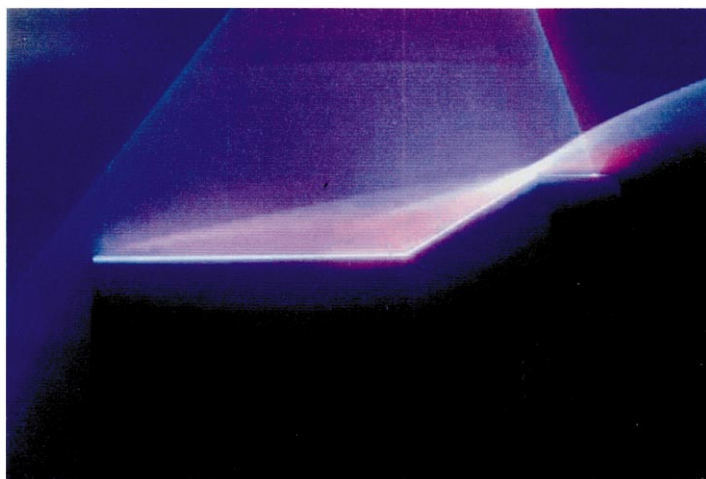


FIGURE 8.3.35 The hollow cylinder-flare model for assessment of code accuracy on a laminar high Mach number interaction (Chanetz *et al.*, 1998).

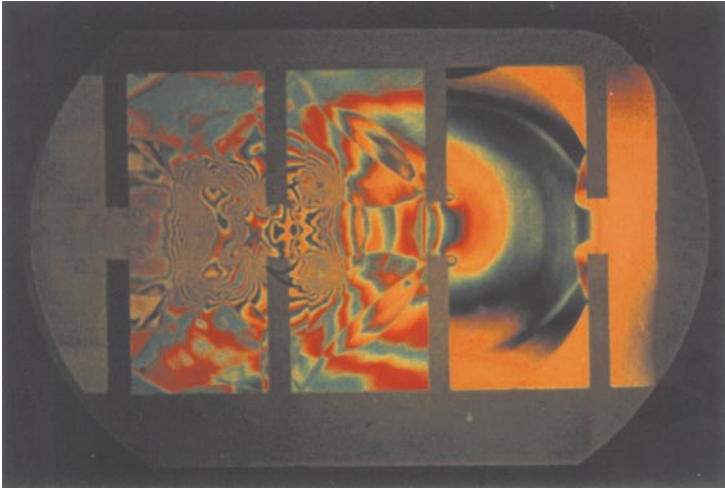


FIGURE 10.9 The process shown in Fig. 10.8 at a later time instant; now it is shown as an interferogram.

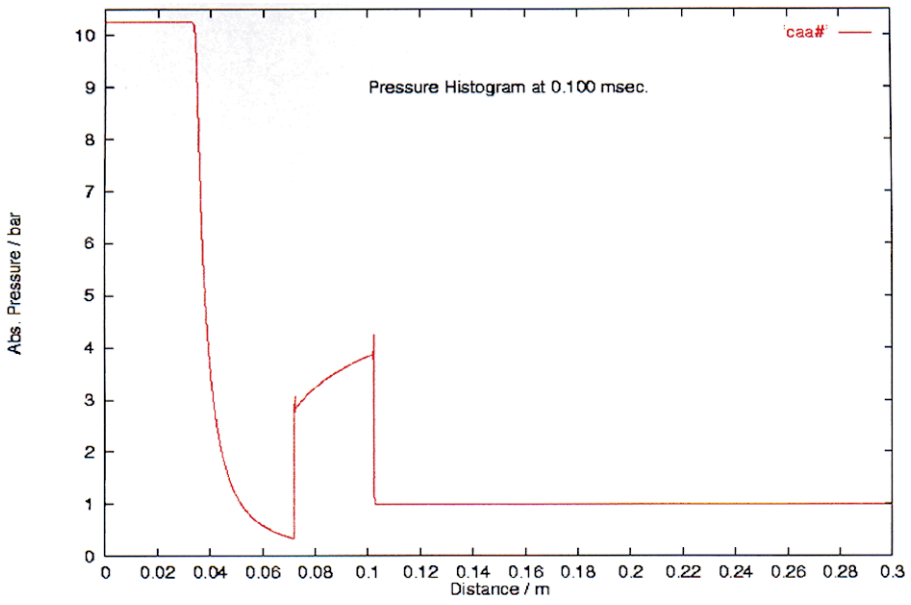
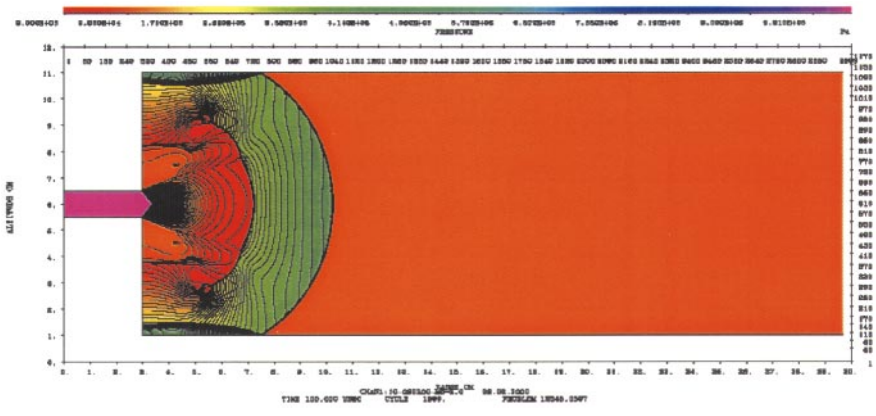


FIGURE 10.42 SHAMRC's isobars and pressure histograms (along the plane of symmetry; $y = 6$ cm) for the propagation of the transmitted shock wave ($M_0 = 3.0$) through an abrupt channel enlargement. The area ratio is 1 : 10. The figure shows the state of the flow (a) 100 μ sec, (b) 200 μ sec, and (c) 400 μ sec after flow initiation. The shock position at initiation time ($t = 0$ μ sec) is $x = 2.5$ cm.

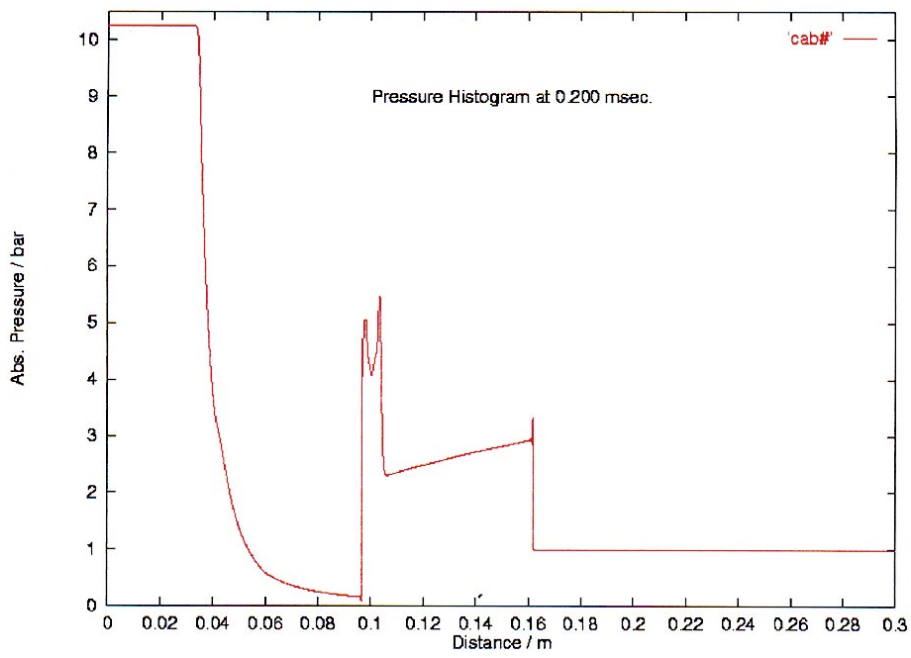
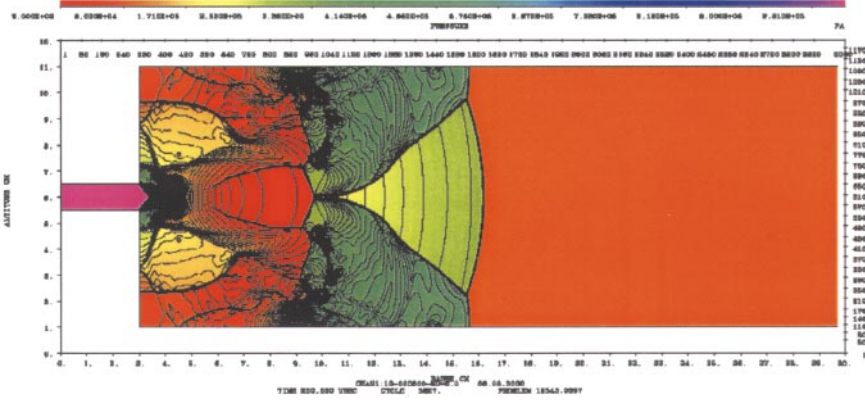


FIGURE 10.42 (continued)

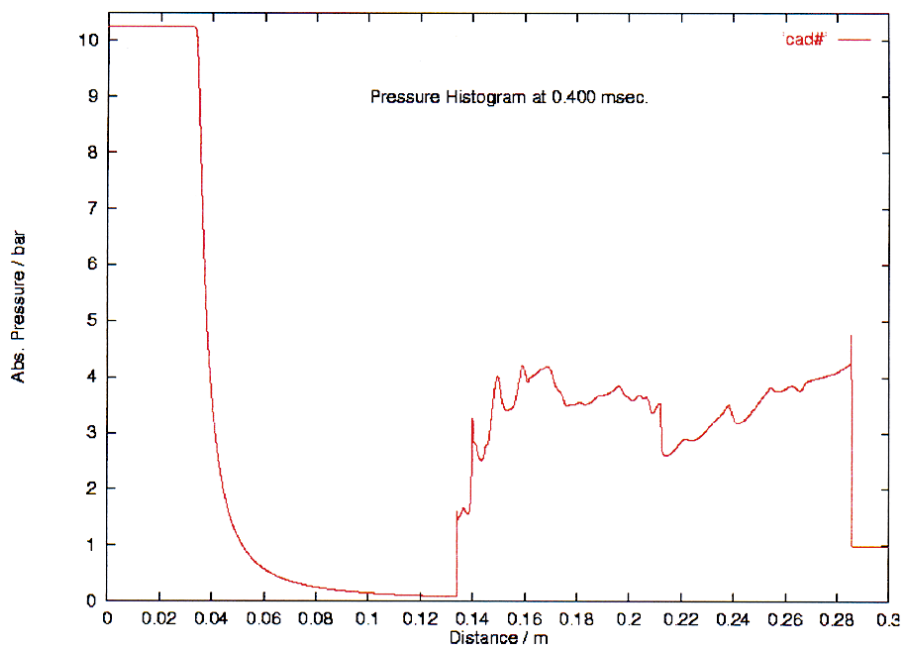
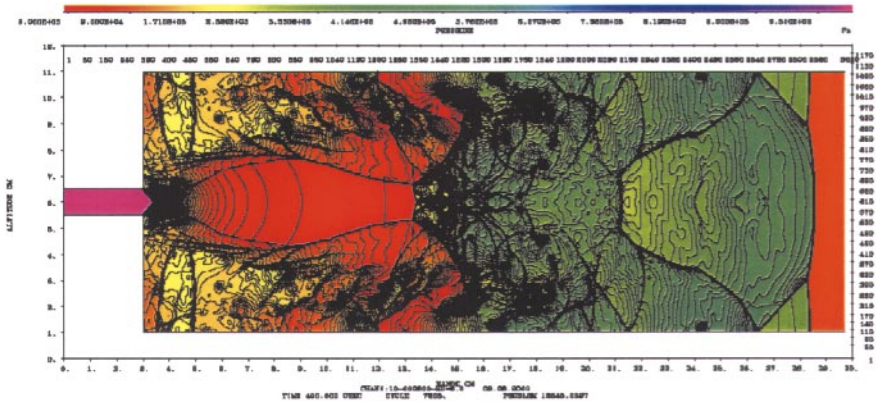


FIGURE 10.42 (continued)

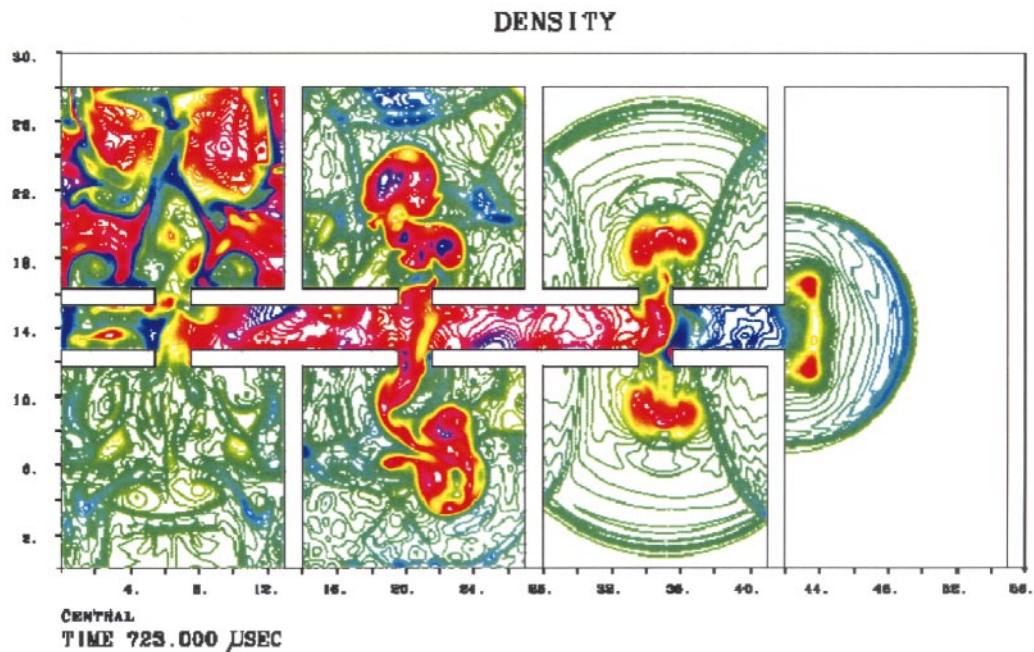


FIGURE 10.44 Isopycnics resulting from the propagation of a detonation wave (blast wave) in a multichamber system (2D). Rooms with a door are connected through a corridor. The wave is “numerically” initiated using a built-in option of SHAMRC by specifying a certain amount of a selectable explosive.